Surgical and Radiologic Anatomy (2026) 48:19
https://doi.org/10.1007/s00276-025-03795-6

ORIGINAL ARTICLE

Optic nerve course and its association with lateral lamella: relevance for endoscopic sinus surgery

Tugba Tulaci[1] · Kamil Gokce Tulaci[1] · Hasan Canakci[1] · Ece Onay Ozgur[1] · Samet Mecit Sengül[2] · Emrah Akay[2] · Omer Hizli[1]

Received: 5 September 2025 / Accepted: 24 November 2025

Abstract

Purpose To investigate the association between the anatomical course of the optic nerve within the sphenoid and posterior ethmoid sinuses (Delano classification) and anterior skull base morphology, particularly lateral lamella length and olfactory fossa depth.

Methods Paranasal sinus CT scans from 192 patients (384 hemi-sinuses) were retrospectively reviewed. The course of the optic nerve was categorized using the Delano classification (types 1–4). Lateral lamella length and Keros classification were assessed for each case. Statistical comparisons were performed using ANOVA, post-hoc Tukey tests, and Chi-square analysis.

Results Lateral lamella length significantly differed among the Delano types ($p=0.001$). Delano type 3 and type 4 sinuses demonstrated significantly longer lateral lamella compared to type 1 ($p=0.026$ and $p=0.016$, respectively). Additionally, a significant variation in Keros classification was observed across Delano groups ($p=0.025$), with higher Delano types showing increased prevalence of Keros type 3. These findings suggest that optic nerve protrusion is associated with elongation of the lateral lamella and deepening of the olfactory fossa.

Conclusion This is the first study to demonstrate a significant anatomical correlation between Delano classification and anterior skull base morphology. As optic nerve protrusion into the sphenoid sinus increases, adjacent skull base structures—particularly the lateral lamella—become elongated, potentially heightening the risk of iatrogenic injury during endoscopic sinus surgery. Combined use of Keros and Delano classifications in preoperative imaging may enhance surgical risk stratification and improve patient safety.

Keywords Paranasal sinuses · Optic nerve · Lateral lamella · Keros classification

✉ Omer Hizli
omerhizli@balikesir.edu.tr

Tugba Tulaci
tugbatulaci@gmail.com

Kamil Gokce Tulaci
ktulaci@gmail.com

Hasan Canakci
hsn_canakci@hotmail.com

Ece Onay Ozgur
eceonayozgur@gmail.com

Samet Mecit Sengül
samet.mecit.sengul@gmail.com

Emrah Akay
emrahakay@hotmail.com

[1] Department of Otorhinolaryngology–Head and Neck Surgery, Faculty of Medicine, Balikesir University, Balikesir, Turkey

[2] Department of Radiology, Faculty of Medicine, Balikesir University, Balikesir, Turkey

Published online: 08 December 2025

Introduction

Functional endoscopic sinus surgery (FESS) is the preferred surgical approach for managing paranasal sinus diseases that are unresponsive to medical therapy. One of the important factors directly affecting the success of FESS is a detailed radiologic evaluation before the operation. During the surgical planning process, detailed evaluation of critical areas such as the anterior skull base, adjacent orbital structures, and neurovascular relationships using high-resolution imaging methods is of great importance to prevent complications [10, 17].

Serious complications can occur in surgical procedures that are not carefully planned and where anatomical variations are overlooked. One of these serious complications is anterior skull base trauma resulting in cerebrospinal fluid (CSF) fistula. The most common area of trauma that can cause CSF fistula is the lateral lamella of the cribriform plate due to its fragile structure [17]. The longer the lateral lamella, the greater likelihood of iatrogenic damage, underscoring the importance of a careful preoperative assessment in this region [18].

One of the primary challenges in preoperative radiologic assessment and surgical execution of FESS arises from considerable individual anatomical variability in the paranasal sinuses, primarily due to differences in pneumatization and other structural variations. A review of the literature on various structural variations and pneumatization differences reveals that most studies have focused on the presence of Onodi cells, skull base asymmetries, frontal cell types, sphenoid sinus pneumatization patterns, and dehiscence of intra-sinus bony structures [1, 15, 16, 23]. However, it is noteworthy that the anatomical course of the optic nerve in the sphenoid and posterior ethmoid sinuses and its relationship with anterior skull base depth and especially lateral lamella length have not been investigated so far.

Therefore, the aim of this radio-anatomical study was to investigate the relationship between the anatomical course of the optic nerve in the sphenoid and posterior ethmoid sinuses and the anterior skull base structures—particularly the lateral lamella—and to assess the surgical relevance of these associations.

Materials and methods

Study design

This retrospective research was carried out in line with the principles outlined in the Declaration of Helsinki. Ethical approval was granted by the Health Sciences Ethics Committee of Balıkesir University (approval number: 2025/8). This study was conducted at the Departments of Otorhinolaryngology and Radiology in Balıkesir University, Faculty of Medicine. Paranasal sinus computed tomography (PNsCT) images were retrieved from the Picture Archiving and Communication System (PACS) of the Balıkesir University.

Power analysis

In order to evaluate whether there is a significant difference between the mean lateral lamella lengths of the patients categorized according to the Delano classification by ANOVA test, the calculation was made using the G power 3.1.9 program, and it was concluded that a minimum of 180 participants was required with a medium effect size (effect sizes for ANOVA according to Cohen: f = 0.25 = medium effect size, (Cohen, 2013), type I error (α) = 0.05, type II error (power or 1-β) = 0.80, the minimum sample size was found to be 180.

All PNsCT scans between January 2020 and January 2025 were reviewed, and the images of 192 patients (79 males and 113 females) who met the inclusion criteria were included in the analysis.

The inclusion criteria were as follows: age ≥ 18 years, no history of facial trauma or sinus surgery, absence of maxillofacial deformity or imaging artefacts.

Patients were excluded from the study if they had conditions that could potentially alter the normal anatomy of the paranasal sinuses, including a history of facial trauma, paranasal sinus neoplasms, inverted papilloma, cystic fibrosis, nasal polyposis, or any prior sinus surgery.

PNsCT imaging and analysis

All paranasal sinus CT scans were performed using standardized imaging protocols, with patients positioned in the supine position. Neither contrast agents nor sedation were utilized during the scanning process.

Imaging was carried out using a 64-slice multidetector CT scanner (Toshiba Aquillon 64, Otawara, Japan). Axial images were acquired from the level of the frontal sinus apex down to the posterior aspect of the hard palate.

The imaging parameters were as follows: slice thickness of 0.5 mm, interslice spacing of 0.3 mm, tube voltage set at 120 kV, and tube current at 150 mA. On average, each scan yielded between 300 and 350 slices. Multiplanar reconstructions (axial, coronal, and sagittal) were generated using both bone and soft tissue algorithms via the Extreme PACS General Radiology Interface.

Evaluations and measurements on PNsCT

Onodi cell: The radiological criterion for defining the Onodi cell (OC) was the presence of a posterior ethmoid air cell

Table 1 Comparison of lateral lamella length (mm) among the groups

		Lateral lamella length (mm) Mean ± Standard deviation
Delano group	Type 1	5.3 ± 1.9
	Type 2	5.9 ± 2
	Type 3	6.1 ± 1.7
	Type 4	6.5 ± 2.6
p value (One way ANOVA)	0.001	

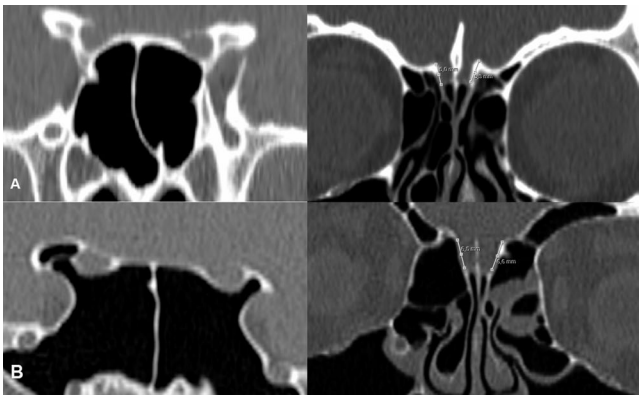

Fig. 1 Comparison of lateral lamella length between Delano type 1 and type 4 sinuses. **A** Lateral lamella length measured as 5.6 mm (right) and 5.3 mm (left) in the Delano Type 1 sinus. **B** Lateral lamella length measured as 6.5 mm (right) and 6.6 mm (left) in the Delano Type 4 sinus

extending superiorly into the sphenoid sinus and partially surrounding the optic canal. Evaluation was performed on coronal CT slices and scored as 0 (absent) or 1 (present).

Delano classification: The anatomical relationship between the optic nerve and the sphenoid sinus was evaluated based on the criteria outlined in the Delano classification [7, 8].

Type 1—Optic nerve is immediately adjacent to lateral and superior wall of sphenoid sinus without impression on sinus wall.

Type 2—Optic nerve causes an impression on lateral sphenoidal sinus wall.

Type 3—Optic nerve courses through the sphenoid sinus.

Type 4—Optic nerve courses immediately lateral to posterior ethmoid and sphenoid sinuses.

Keros classification of olfactory fossa: Measurements of the ethmoid roof were performed on coronal CT images using consistent anatomical landmarks [5]. These points were defined as the medial ethmoid roof—the junction where the ethmoid roof meets the lateral lamella medially—and the cribriform plate point. The depth of the olfactory fossa was determined by measuring the perpendicular distance from the medial ethmoid roof to the cribriform plate plane [2, 9]. According to the classification system introduced by Keros [19] this depth is categorized based on the height of the lateral lamella: Type I corresponds to a depth of 1–3 mm, Type II to 4–7 mm, and Type III to 8–16 mm [20].

Lateral lamella length: In accordance with the existing literature, we measured lateral lamella length as the lateral boundary of the cribriform plate between the horizontal cribriform plate and fovea ethmoidalis [10].

Statistical analysis

Study findings were expressed as mean ± standard deviation (SD). The normality of data distribution was assessed using the Kolmogorov–Smirnov test, (p = 0.086). To compare the length of the lateral lamella (LL) across the four groups, a one-way analysis of variance (ANOVA) was applied. Homogeneity of variances was investigated employing Levene test (p = 0.292). For post-hoc comparisons, Tukey test was used.

The distribution of Keros types among the different Delano classification groups was analyzed using the Chi-square test. All statistical evaluations were conducted using SPSS software version 30.0 for MacOS (SPSS Inc., Chicago, IL, USA). A p-value below 0.05 was accepted as the threshold for statistical significance.

Results

In total, 384 hemi-sinuses on CT scans from 192 patients (79 males and 113 females, mean age: 32.3 ± 11.7 years) were included in the study. Relationship of optic nerves to the sphenoid and posterior ethmoid sinuses were categorized based on Delano classification. Delano type 1 group consisted of 222, type 2 group consisted of 76, type 3 group consisted of 58 and type 4 group consisted of 28 optic nerves.

Comparison of lateral lamella length (mm) among the Delano groups was presented in Table 1. According to one-way ANOVA, LL length showed a statistically significant difference across the four Delano groups ($p = 0.001$). Post-hoc pairwise comparisons (Tukey test) revealed that, no significant difference in LL length was evident between Delano type 1 and 2 ($p = 0.175$), between Delano type 2 and 3 ($p = 0.841$), between Delano type 3 and 4 ($p = 0.86$), and between Delano type 2 and 4 sphenoid sinuses ($p = 0.455$). However, LL length was significantly higher in Delano type 4 sphenoid sinuses compared to type 1 sphenoid sinuses ($p = 0.016$) (Fig. 1). Additionally, LL length was again significantly higher in Delano type 3 sphenoid sinuses compared to type 1 sphenoid sinuses ($p = 0.026$) (Fig. 2).

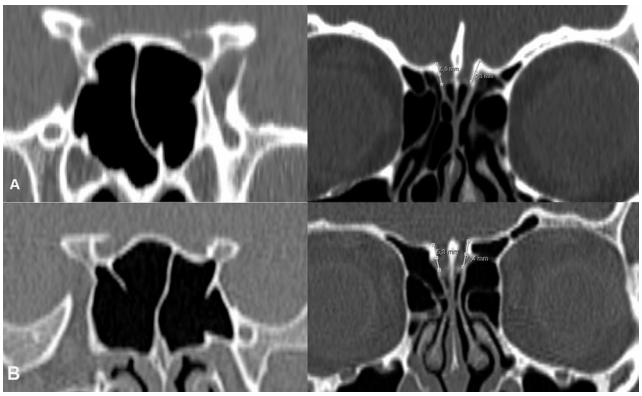

Fig. 2 Comparison of lateral lamella length between Delano type 1 and type 3 sinuses. **A** Lateral lamella length measured as 5.6 mm (right) and 5.3 mm (left) in the Delano Type 1 sinus. **B** Lateral lamella length measured as 6.3 mm (right) and 6.4 mm (left) in the Delano Type 3 sinus

Table 2 Keros distribution of Delano groups

	Keros classification			
	1 n (%)	2 n (%)	3 n (%)	Total n (%)
Delano Type 1	59 (26.6%)	127 (57.2%)	36 (16.2%)	222 (100%)
Delano Type 2	12 (15.8%)	46 (60.5%)	18 (23.7%)	76 (100%)
Delano Type 3	7 (12.1%)	39 (67.2%)	12 (20.7%)	58 (100%)
Delano Type 4	1 (3.6%)	21 (75%)	6 (6%)	28 (100%)
P value (Chi-square)	0.025			

n = Number of hemi-sinuses

Table 2 presents the Keros distribution of Delano groups. A significant difference of Keros distribution was evident across Delano groups ($p = 0.025$, $X^{2=}$ 14.47). Among the 28 hemi-sinuses classified as Delano Type 4, 1 (3.6%) was identified as Keros Type 1, whereas in the 222 hemi-sinuses classified as Delano Type 1, 59 (26.6%) were categorized as Keros Type 1.

Discussion

In this study, we aimed to investigate the anatomical relationship between the course of the optic nerve within the sphenoid and posterior ethmoid sinuses and anterior skull base structures, particularly the lateral lamella. To the best of our knowledge, no previous study has systematically examined the spatial association between the optic nerve and key anterior skull base structures.

Our results demonstrated a notable correlation: as the Delano classification progressed from Type 1 to Type 4 -indicating increased proximity or protrusion of the optic nerve into the sphenoid sinus- both the mean length of the lateral lamella and the depth of the olfactory fossa increased. This correlation carries important surgical implications. The lateral lamella, which forms the lateral boundary of the cribriform plate, is considered the thinnest and most vulnerable segment of the anterior skull base. Especially in cases where the optic nerve is closely associated with the sphenoid sinus (Delano type 4), the additional presence of a long lateral lamella may reflect an altered skull base configuration that is more susceptible to intraoperative injury during FESS.

Our findings indicate that the coexistence of advanced Delano types and elongated lateral lamella morphology may represent a multiplicative rather than an additive risk factor in endoscopic sinus surgery. While optic nerve protrusion alone is a well-recognized danger zone for potential injury, its concurrent presence with a long lateral lamella and a deep olfactory fossa creates a compounded anatomical vulnerability. In this context, surgeons are not only facing the risk of direct optic nerve trauma but also an increased likelihood of cerebrospinal fluid leakage due to lateral lamella fragility. This dual hazard profile suggests that careful recognition of these combined risk factors during preoperative planning is essential for preventing severe complications.

From a clinical standpoint, such anatomical constellations may influence surgical strategy. For example, in patients with a Delano type 3–4 optic nerve course accompanied by a Keros type II–III configuration, surgeons may need to adopt a more conservative dissection technique, limit unnecessary drilling, and prioritize intraoperative navigation when available. Even in operating rooms where CT images are routinely accessible, standardized preoperative measurements of optic nerve course, lateral lamella length, and olfactory fossa depth can provide surgeons with a structured risk map that guides intraoperative decisions. Beyond identifying optic nerve protrusion alone, acknowledging the combined anatomical variations allows for a more nuanced, patient-specific risk assessment that may help reduce the risk of severe complications such as optic nerve damage or CSF fistula.

An additional important implication of our findings is their potential to contribute to the improvement of existing radiologic risk classification systems. While the Keros classification remains a widely used and valuable tool for assessing the risk of cerebrospinal fluid (CSF) leakage based on olfactory fossa depth, it does not account for anatomical variations in the course of the optic nerve [6, 12, 14]. In contrast, the Delano classification grades the protrusion or dehiscence of the optic nerve into the sphenoid sinus; however, this system may also have limitations when used solely [4, 22]. Our findings suggest that a preoperative risk assessment approach combining both the Keros and Delano

classifications may offer a more comprehensive understanding of anterior skull base anatomy and improve the prediction of intraoperative complications.

Our findings also support the notion that postnatal pneumatization of the sphenoid sinus plays a role in shaping the development of the skull base [3, 21]. From an embryological perspective, the optic nerve originates from the diencephalon, while the anterior skull base -including the ethmoid and sphenoid bones- develops from surrounding mesenchymal tissue. During the postnatal period, sphenoid sinus pneumatization progresses in a variable manner, potentially influencing the final spatial configuration of adjacent neurovascular and bony structures [3]. The findings of our study suggest that in cases of advanced lateral pneumatization of the sphenoid sinus -such as in higher Delano types- there may also be a vertical elongation of the lateral lamella. This may be due to compensatory changes in the morphology of the anterior skull base.

In the existing literature on the optic nerve and sphenoid sinus, most studies have concentrated on anatomical variations involving adjacent structures—such as protrusion or dehiscence of the carotid canal, Vidian canal, foramen rotundum, or anterior clinoid process, rather than their relationship with anterior skull base morphology [13, 17]. However, they have not quantitatively evaluated the relationship between the position of the optic nerve and skull base structures such as the lateral lamella or olfactory fossa. In this context, our study uniquely examines the correlation between the course of the optic nerve and key anterior skull base features, such as the olfactory fossa depth and the lateral lamella length, offering new insights into surgical risk assessment. To our knowledge, this is the first study to quantitatively demonstrate a direct anatomical link between Delano classification types and lateral lamella morphology, bridging a gap in current literature.

From a clinical perspective, the findings of this study highlight the importance of a comprehensive preoperative radiologic evaluation of the optic nerve course. This includes not only its relationship with the sphenoid sinus and the Onodi cell, but also its association with lateral lamella length and olfactory fossa depth. These insights offer a more holistic anatomical perspective for both radiologists and endoscopic surgeons.

Systems such as the Keros classification have long been used to predict the risk of cerebrospinal fluid (CSF) leakage and other surgical complications by classifying skull base depth according to the height of the lateral lamella [11, 22]. Our findings suggest that the Delano classification may also serve as an additional assessment tool for classifying surgical risks. The combined integration of the Keros and Delano classifications into preoperative planning may allow surgeons to more comprehensively evaluate the risks in the anterior skull base region. For instance, in a patient with a Keros Type III skull base (deeper olfactory fossa) and a Delano Type 4 optic nerve, the risks of both cerebrospinal fluid leakage and optic nerve injury may be significantly elevated. In such cases, surgeons should proceed with particular care during endoscopic sinus or transsphenoidal procedures, tailoring their surgical approach to the specific anatomical risk profile of the patient.

Viewed from an alternative perspective, our findings imply that patients with a longer lateral lamella may also have higher Delano scores, reflecting a closer anatomical proximity between the optic nerve and the sphenoid or posterior ethmoid sinuses. In this context, lateral lamella length should be considered not only as a predictor of cerebrospinal fluid leakage, but also as a potential marker for an increased risk of optic nerve injury.

One limitation of our study is the unequal distribution of cases among Delano groups, with a predominance of Type 1 ($n=222$) and relatively fewer instances of Type 4 ($n=28$) hemi-sinuses. This imbalance likely reflects the naturally lower prevalence of Type 4 optic nerve configuration in the general population. Given the unequal distribution of cases and the small number of Type 4 cases in our study, these findings should be interpreted with caution and validated in larger, multicenter studies.

Future multicenter studies with larger sample sizes, combined with the integration of three-dimensional imaging techniques, may help validate our findings across diverse populations. Moreover, prospective clinical trials investigating the association between Keros–Delano anatomical profiles and surgical complication rates could provide clearer insight into the real-world value of these markers in enhancing surgical safety.

Conclusion

This study demonstrated a significant anatomical association between the course of the optic nerve within the sphenoid sinus, as classified by Delano types, and the vertical architecture of the anterior skull base, particularly the lateral lamella length. As the degree of optic nerve protrusion into the sphenoid sinus increased (from Delano Type 1 to Type 4), a corresponding increase in lateral lamella length was observed. This finding suggests that advanced sphenoid sinus lateral pneumatization not only alters the optic nerve's anatomical trajectory but may also contribute to elongation of adjacent skull base structures. Given the vulnerability of the lateral lamella during endoscopic sinus surgery, this correlation may represent an important radiological marker for predicting surgical risk. Incorporating both Delano and Keros classifications into preoperative evaluation may allow

for more comprehensive risk stratification, particularly in anatomically complex cases. A limitation of this study is the relatively small sample size of Delano Type 4 cases ($n=28$), which may limit the generalizability of these findings. Further studies with larger and more diverse samples are needed to validate these results across different populations.

Author contributions Protocol/project development: OH, KGT, Data collection or management: SMS, EA, HÇ, Data analysis: OH, TT, KGT, EOO, Manuscript writing/editing: OH, KGT, HÇ. All authors reviewed the manuscript.

Funding This study did not receive funding.

Data availability No datasets were generated or analysed during the current study.

Declarations

Conflict of interest The authors declare no competing interests.

Ethical approval All procedures performed in studies involving human participants were in accordance with the ethical standards of the Health Sciences Ethics Committee of Balıkesir University (approval number: 2025/8) and with the 1964 Helsinki declaration and its later amendments or comparable ethical standards.

Informed consent Informed consent was obtained from all individual participants included in the study.

References

1. Açar G, Gökşan AS, Aydoğdu D (2024) Computed tomography based evaluation of the association between sphenoid sinus pneumatization patterns and variations of adjacent bony structures in relation to age and gender. Neurosurg Rev 47(1):349. https://doi.org/10.1007/s10143-024-02594-8
2. Alazzawi S, Omar R, Rahmat K, Alli K (2012) Radiological analysis of the ethmoid roof in the malaysian population. Auris Nasus Larynx 39(4):393–396. https://doi.org/10.1016/j.anl.2011.10.002
3. Cellina M, Gibelli D, Floridi C, Toluian T, Valenti Pittino C, Martinenghi C, Oliva G (2020) Sphenoid sinuses: pneumatisation and anatomical variants-what the radiologist needs to know and report to avoid intraoperative complications. Surg Radiol Anat 42(9):1013–1024. https://doi.org/10.1007/s00276-020-02490-y
4. DeLano MC, Fun FY, Zinreich SJ (1996) Relationship of the optic nerve to the posterior paranasal sinuses: a ct anatomic study. AJNR Am J Neuroradiol 17(4):669–675
5. Dessi P, Castro F, Triglia JM, Zanaret M, Cannoni M (1994) Major complications of sinus surgery: a review of 1192 procedures. J Laryngol Otol 108(3):212–215. https://doi.org/10.1017/s0022215100126325
6. Heaton CM, Goldberg AN, Pletcher SD, Glastonbury CM (2012) Sinus anatomy associated with inadvertent cerebrospinal fluid leak during functional endoscopic sinus surgery. Laryngoscope 122(7):1446–1449. https://doi.org/10.1002/lary.23305
7. Hiremath SB, Gautam AA, Sheeja K, Benjamin G (2018) Assessment of variations in sphenoid sinus pneumatization in Indian population: a multidetector computed tomography study. Indian J Radiol Imaging 28(3):273–279. https://doi.org/10.4103/ijri.IJRI_70_18
8. Kanotra S, Bashir S, Sharma P, Purbi S, Manzoor M, Gupta K (2023) Anatomical variations of the optic nerve in the sphenoid sinus: do ethnic variations matter? Indian J Otolaryngol Head Neck Surg 75(3):1943–1949. https://doi.org/10.1007/s12070-023-03798-y
9. Kaplanoglu H, Kaplanoglu V, Dilli A, Toprak U, Hekimoğlu B (2013) An analysis of the anatomic variations of the paranasal sinuses and ethmoid roof using computed tomography. Eurasian J Med 45(2):115–125. https://doi.org/10.5152/eajm.2013.23
10. Kayabasi S, Hizli O, Ozkan D (2019) Does paranasal sinus development affect olfactory fossa depth and lateral lamella length? Laryngoscope 129(11):2458–2463. https://doi.org/10.1002/lary.27940
11. Keros P (1962) on the practical value of differences in the level of the lamina cribrosa of the ethmoid. Zeitschrift fur Laryngologie, Rhinologie, Otologie und ihre Grenzgebiete. 1(41):809–813
12. Lebowitz RA, Terk A, Jacobs JB, Holliday RA (2001) Asymmetry of the ethmoid roof: analysis using coronal computed tomography. Laryngoscope 111(12):2122–2124. https://doi.org/10.1097/00005537-200112000-00007
13. Liu J, Liu Q, Wang N (2019) Posterior ethmoid cell expansion towards the inferolateral region of the sphenoid sinus: a computed tomography study. Surg Radiol Anat 41(9):1011–1018. https://doi.org/10.1007/s00276-019-02277-w
14. Meyers RM, Valvassori G (1998) Interpretation of anatomic variations of computed tomography scans of the sinuses: a surgeon's perspective. Laryngoscope 108(3):422–425. https://doi.org/10.1097/00005537-199803000-00020
15. Ozcan KM, Hizli O, Sarisoy ZA, Ulusoy H, Yildirim G (2018) Coexistence of frontal sinus hypoplasia with maxillary sinus hypoplasia: a radiological study. Eur Arch Otorhinolaryngol 275(4):931–935. https://doi.org/10.1007/s00405-018-4892-9
16. Ozturan O, Yenigun A, Degirmenci N, Aksoy F, Veyseller B (2013) Co-existence of the onodi cell with the variation of perisphenoidal structures. Eur Arch Otorhinolaryngol 270(7):2057–2063. https://doi.org/10.1007/s00405-012-2325-8
17. Sancar B, Duman SB (2022) Olfactory fossa evaluation as a maxillary sinus development using cone beam computed tomography. Indian J Otolaryngol Head Neck Surg 74(Suppl 2):1566–1570. https://doi.org/10.1007/s12070-021-02700-y
18. Solares CA, Lee WT, Batra PS, Citardi MJ (2008) Lateral lamella of the cribriform plate: software-enabled computed tomographic analysis and its clinical relevance in skull base surgery. Arch Otolaryngol Head Neck Surg 134(3):285–289. https://doi.org/10.1001/archotol.134.3.285
19. Hr S (1995) Paranasal sinuses: Anatomic terminology and nomenclature. Ann Otol Rhinol Laryngol Suppl 167:7–16
20. Stankiewicz JA (1989) Complications of endoscopic sinus surgery. Otolaryngol Clin North Am 22(4):749–758
21. Vidić B (1968) The postnatal development of the sphenoidal sinus and its spread into the dorsum sellae and posterior clinoid processes. AJR Am J Roentgenol 104(1):177–183. https://doi.org/10.2214/ajr.104.1.177
22. Yazici D (2019) The analysis of computed tomography of paranasal sinuses in nasal septal deviation. J Craniofac Surg 30(2):e143–e147. https://doi.org/10.1097/scs.0000000000005077
23. Yazici D (2019) The effect of frontal sinus pneumatization on anatomic variants of paranasal sinuses. Eur Arch Otorhinolaryngol 276(4):1049–1056. https://doi.org/10.1007/s00405-018-5259-y